

Electronic Spectroscopy of UO_2 Isolated in a Solid Ar Matrix

Christopher J. Lue, Jin Jin, Mariana J. Ortiz, Jonathan C. Rienstra-Kiracofe, and Michael C. Heaven*

Contribution from the Department of Chemistry, Emory University, Atlanta, Georgia 30322

Received October 8, 2003; E-mail: heaven@euch4e.chem.emory.edu

Abstract: Dispersed fluorescence spectra have been recorded for UO_2 isolated in a solid Ar matrix. Near UV excitation produced groups of emission bands in the 370–420 and 465–645 nm spectral regions. These bands originated from two energetically close upper levels and terminated on a range of low-lying electronic states. Comparisons with electronic structure calculations indicate that the ground and low-lying electronic states of UO_2 are derived from the $\text{U}(5f7s)$ configuration. The level of agreement between the observed and predicted electronic energies provides an impressive validation of the calculations. In previous studies of matrix isolated UO_2 , it had been suggested that the ground state in solid Ar is $\text{U}(5f^2) \ ^3\text{H}$. The present results do not appear to be consistent with this hypothesis.

Introduction

Quantum chemistry calculations are now reaching a level of sophistication where they may provide accurate results for simple lanthanide and actinide compounds. These advances offer the possibility that actinide chemistry may soon be explored by computational methods, thereby circumventing many hazardous and expensive experimental studies. At this point, it is essential to evaluate the results obtained using various methods for incorporating relativistic terms in quantum chemistry calculations. Spectroscopic measurements for isolated molecules provide the best data for comparison, but there have been very few gas-phase studies of actinide compounds. In principle, studies of molecules isolated in rare gas matrices should also provide critical benchmark data. However, there are subtle complications that must be taken into account when interpreting the data for actinide compounds obtained from cryogenic matrices. Andrews and co-workers^{1–4} have studied a range of uranium compounds trapped in rare gas matrices. For the molecules UO , UO_2 , and CUO , they observed anomalously large changes in vibrational frequencies when the host material was changed from Ne to Ar. For example, the antisymmetric stretch of UO_2 was observed at 914 cm^{-1} in Ne and 776 cm^{-1} in Ar.^{2,4} Zhou et al.² used density functional theory (DFT) to investigate the cause of this large effect. Their calculations were the first to indicate that UO_2 has a $^3\Phi$ ground state derived from the $\text{U}(5f7s)$ configuration. Prior studies had concluded that the ground state was ^3H , derived from $\text{U}(5f^2)$. Zhou et al.² found that the calculated vibrational frequency for the $^3\Phi$ state corresponded to the Ne matrix result, while the frequency for the ^3H state agreed with the Ar matrix data. Consequently, they proposed that the guest–host interaction in Ar reversed the

energy ordering of the $^3\Phi$ and ^3H states. Similarly, it has been proposed that the interaction between CUO and Ar is large enough to reorder the low-lying electronic states.^{5–6} On the basis of the results from DFT calculations, Li et al.⁶ concluded that the rare gas atoms Ar, Kr, and Xe form weak chemical bonds with CUO . An implication of these studies is that calculations that are to be evaluated against matrix data will need to include an explicit treatment of the guest–host interactions.

In the present study, we have examined the electronic emission spectrum of UO_2 trapped in solid Ar. The objective was to characterize the low-lying electronic states and thereby determine the electronic configuration for the ground state. As recent gas-phase measurements⁷ confirm that the ground state of UO_2 is $\text{U}(5f7s) \ \text{X}^3\Phi_{2u}$, we were particularly interested to see if the electronic emission spectrum for UO_2 in Ar would show evidence of state reordering. In addition, we have used the matrix emission spectrum to assess the quality of recent ab initio predictions^{8–10} for the low-lying electronic states of UO_2 .

Experimental Section

The matrix isolation unit used for this work has been described previously.¹¹ Uranium dioxide was obtained in the gas phase by laser vaporization of a uranium metal target. The second harmonic from an Nd:YAG laser was used for ablation. The laser was operated at approximately 30 mJ per pulse with a repetition frequency of 10 Hz. A 10 cm focal length lens was used to focus the beam on the surface of the metal. In the first series of experiments, the ablated material was carried to the matrix chamber in a flow of Ar that contained 0.1%

- (1) Zhou, M. F.; Andrews, L.; Li, J.; Bursten, B. E. *J. Am. Chem. Soc.* **1999**, *121*, 9712.
- (2) Zhou, M. F.; Andrews, L.; Ismail, N.; Marsden, C. *J. Phys. Chem. A* **2000**, *104*, 5495.
- (3) Tauge, J. T., Jr.; Andrews, L.; Hunt, R. D. *J. Phys. Chem.* **1993**, *97*, 10920.
- (4) Hunt, R. D.; Andrews, L. *J. Chem. Phys.* **1993**, *98*, 3690.

- (5) Andrews, L.; Liang, B.; Li, J.; Bursten, B. E. *J. Am. Chem. Soc.* **2003**, *125*, 3126.
- (6) Li, J.; Bursten, B. E.; Liang, B.; Andrews, L. *Science* **2002**, *295*, 2242.
- (7) Han, J.; Kaledin, L. A.; Goncharov, V.; Komissarov, A. V.; Heaven, M. C. *J. Am. Chem. Soc.* **2003**, *125*, 7176.
- (8) Gagliardi, L.; Roos, B. O.; Malmqvist, P.; Dyke, J. M. *J. Phys. Chem. A* **2001**, *105*, 10602.
- (9) Majumdar, D.; Balasubramanian, K.; Nitsche, H. *Chem. Phys. Lett.* **2002**, *361*, 143.
- (10) Chang, Q. Ab Initio Calculations on UO_2 . Masters Thesis, Ohio State University, Columbus, 2002 (Research advisor, R. M. Pitzer).
- (11) Nicolai, J. P.; Heaven, M. C. *J. Chem. Phys.* **1987**, *87*, 3304.

O_2 . This mixture was chosen as it provided optimal yields of UO_2 in previous laser ablation studies.^{2,4} However, the target used in our matrix experiments was so heavily oxidized that good yields of UO_2 could be obtained without adding O_2 to the carrier flow. The UO_3/Ar mixture was deposited on a copper mirror that was cooled to 12 K by a closed-cycle He refrigerator. Typically, the samples were accumulated for 3 h, at an Ar flow rate of approximately 5 mmol/h.

After deposition, the matrices were excited using light from various pulsed laser sources. Fixed wavelength excitation was carried out using the third or fourth harmonic from a Nd:YAG laser (355 and 266 nm), or the 308 nm light from a XeCl excimer laser. Tunable dye lasers were used to excite the matrices in the 358–388, 336–358, and 560–580 nm ranges. The near UV wavelengths were obtained from an excimer-pumped dye laser (Labda Physik EMG101/FL3002E), and visible light was provided by an Nd:YAG pumped dye laser (Quanta Ray DCR2A/PDL1).

Fluorescence from the matrix was collected by a collimating lens and focused through the entrance slits of a 0.64 m monochromator (ISA, 1200 lines/mm grating). In most experiments, long-pass filters were used to block laser scatter. Fluorescence was detected by a photomultiplier tube (Thorn EMI 9558QB). Signals were recorded using a digital oscilloscope (LeCroy ScopeStation 140) or boxcar integrator (SRS model 250) interfaced to a personal computer. A 0.4 μs boxcar gate, delayed by 0.3 μs relative to the excitation pulse, was used to record dispersed fluorescence spectra. The monochromator was calibrated using the lines from a Hg emission lamp. Fluorescence decay curves were recorded using the signal averaging capabilities of the digital oscilloscope.

Results

(i) Fixed Wavelength Excitation. Excitation of the matrices at 355, 308, and 266 nm produced an emission spectrum that consisted of a group of resolved features in the 370–420 nm range (Figure 1a), and a broad, unresolved group of bands in the 465–645 nm range (Figure 1b). The band centers for the strongest features of Figure 1a are listed in Table 1. These bands exhibited a line width of 150 cm^{-1} (fwhm), which was broader than the resolution setting of the monochromator (estimated to be 70 cm^{-1} in this wavelength range, based on the width of the scattered laser line when 355 nm excitation was used). It is probable that the resolution of the spectrum was limited by phonon wing broadening. When comparable laser powers were used, 355 nm excitation produced far weaker fluorescence signals than 308 or 266 nm light.

Fluorescence decay curves were recorded for all of the resolved bands in Figure 1a (six different emission wavelengths) and four different regions of the broad emission feature (Figure 1b, 475, 485, 510, and 573 nm). Beyond the scattered laser signals in the 0–100 ns range, the decay curves were single exponential, yielding a common fluorescence decay lifetime of $820 \pm 20\text{ ns}$.

(ii) Tunable Wavelength Excitation. Tunable laser excitation was used to investigate the excited levels that gave rise to the emission bands shown in Figure 1. Wavelength selected fluorescence excitation spectra were recorded by scanning the excitation wavelength while monitoring the light emitted by a specific emission band. The results from our studies of gas-phase UO_2 were used to determine the range of excitation wavelength examined. A scan of the dye laser over the range from 360 to 372 nm, with detection of fluorescence at 390 nm, revealed a single broad excitation feature. This band was centered at 364.0 nm ($27\,470\text{ cm}^{-1}$) with a fwhm of 400 cm^{-1} . The fluorescence decay lifetime of the 390 nm emission was

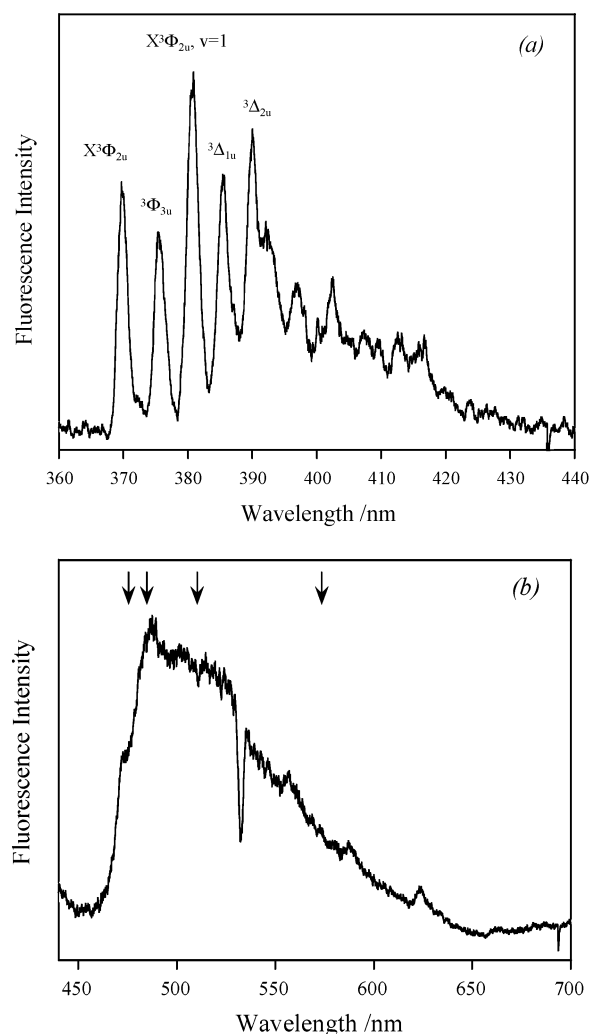


Figure 1. Emission spectra for UO_2 trapped in solid Ar at 12 K. These traces were recorded using 266 nm excitation. (a) Fluorescence in the 360–440 nm range. The term symbols indicate proposed assignments for the lower levels of the resolved bands. (b) Fluorescence in the 440–700 nm range. The negative-going feature at 532 nm was an artifact caused by saturation of the detector by second-order transmission of scattered laser light. The arrows above the spectrum indicate the wavelengths at which fluorescence decay curves were recorded.

Table 1. Band Positions for Matrix Isolated UO_2 and Comparison of Observed Low-Lying Energy Levels with Theoretical Predictions^a

band position	energy	theory ^b	theory ^c	assignment
27 036	0	0	0	$X^3\Phi_{2u}$
26 628	408	431	403	$^3\Phi_{3u}$
26 265	771			$X^3\Phi_{2u}, v = 1$
25 942	1094	1088	1935	$^3\Delta_{2u}$
25 635	1401	1566	2340	$^3\Delta_{1u}$

^a Band position and energies are in units of cm^{-1} . ^b See ref 10. ^c See ref 8.

examined using 364 nm excitation. The beginning of the decay curve was obscured by intense scattered light from the laser that was partially transmitted by the monochromator, but fitting to the tail of the decay signal yielded a lifetime of $120 \pm 30\text{ ns}$.

An excitation spectrum recorded using detection of the visible band emission at 480 nm located two broad absorption features in the 360–372 nm range. One was identical to the feature described above. The second was centered at 380.5 nm ($26\,280\text{ cm}^{-1}$) with a fwhm of 420 cm^{-1} . Fluorescence decay curves

for the 480 nm emission, recorded using 364.0 or 380.5 nm excitation, yielded a lifetime of 90 ± 30 ns.

A scan over the 330–360 nm range, with detection at 390 nm, yielded a broad absorption feature that was centered at 340.0 nm ($29\,410\text{ cm}^{-1}$) with a fwhm of 420 cm^{-1} . The fluorescence decay lifetime was 310 ± 20 ns. The visible emission band system was not present for 340.0 nm excitation.

There were no features in the spectra obtained by UV excitation that could be assigned to U atoms or UO. To test for the presence of these species, we excited the matrices using tunable radiation in the 560–580 nm range. From gas-phase studies, it is known that both U¹² and UO^{13,14} have strong absorption bands in this region. However, these experiments did not yield detectable emission from U or UO.

Analysis and Discussion

Evidence that the emitting species observed in these experiments was UO₂ was drawn from previous matrix experiments and complementary gas-phase studies. Hunt and Andrews⁴ used IR spectroscopy to examine the range of species made by laser ablating uranium metal into Ar/O₂ mixtures and trapping the products. They observed bands of UO, UO₂, and UO₃ in their matrices. We have examined the products produced by laser ablating an oxidized uranium target using mass spectrometry.^{7,15} Under the conditions of our matrix experiments, the products were found to be U, UO, and UO₂. As the visible excitation experiments do not show the presence of significant quantities of U or UO in our samples, it seems most likely that the emitting species is UO₂. This inference is further supported by the observation that the features of the fluorescence excitation spectra and the highest energy emission band recorded in the matrix correlate with a strong absorption feature in the spectrum of gas-phase UO₂. We are currently using resonantly enhanced multiphoton ionization (REMPI) with mass selected ion detection to characterize the electronic spectroscopy of UO₂ (ref 15). The REMPI spectrum shows strong features at 366.85 nm ($27\,260\text{ cm}^{-1}$) and 337.05 nm ($29\,669\text{ cm}^{-1}$). The maximum of the 364 nm matrix band is blue-shifted relative to the gas-phase bands by 210 cm^{-1} , which is typical for an electronic transition of a small molecule isolated in solid Ar.¹⁶ Note that the red edge of the 364 nm band (at approximately 369 nm) overlaps the blue edge of the 370 nm emission feature, which extends to 368.5 nm. This is consistent with a single electronic transition that is phonon broadened (blue-shading on excitation and red-shading on emission). The overlap of the excitation and emission bands indicates that the zero-phonon transition occurs at $27\,120\text{ cm}^{-1}$, just 140 cm^{-1} below the position of the corresponding gas-phase band. The fact that the excitation and emission features overlap indicates that there is some inhomogeneous line broadening due to differences in local trapping sites. The maximum of the 340 nm excitation band red-shifted relative to the corresponding gas-phase band by 260 cm^{-1} . As noted above, this is within the range typically encountered for Ar matrices.

Overall, we find that the pattern of low-lying electronically excited levels of UO₂ revealed by the matrix emission spectrum is in good agreement with the predictions of high-level theoretical calculations^{8,10} (vide infra). It has been established that UO₂ is a linear, symmetric molecule in the ground and low-lying excited states. Ab initio studies of UO₂ excited states have been carried out most recently by Chang¹⁰ and Gagliardi et al.⁸ In agreement with the DFT study by Zhou et al.,² these calculations predict that the lowest energy states are derived from the U (5f7s) configuration. The ground state is $X^3\Phi_{2u}$, with the $^3\Phi_{3u}$ component lying at approximately 420 cm^{-1} higher energy (Han et al.⁷ found that these levels are separated by 368 cm^{-1} in the gas phase). The calculations of Chang¹⁰ and Gagliardi et al.⁸ predict $\Omega = 1u$ and $2u$ levels, derived from the lowest energy $^3\Delta$ state, that lie about 1500 cm^{-1} above the $^3\Phi$ states. This pattern is readily discerned in Figure 1a. Band assignments are given in Table 1, and the theoretically predicted energies are compared with the intervals derived from the spectrum. This assignment scheme carries the implication that the transitions originate from an $\Omega = 2g$ state. The emission band at $26\,265\text{ cm}^{-1}$ terminates on a level that is $771 \pm 10\text{ cm}^{-1}$ above the ground state. This interval is consistent with excitation of the U–O stretch vibration. The asymmetric stretch fundamental of UO₂ in Ar^{4,17} is observed at 776 cm^{-1} . The symmetric stretch has been observed at 728 cm^{-1} for the mixed isomer ¹⁸OU¹⁶O. From this observation, Gabelnick et al.¹⁷ derived a frequency of 765 cm^{-1} for U¹⁶O₂. The uncertainty in the vibrational interval from the emission spectrum is too great for assignment of the symmetry of the stretch mode. However, as it is unlikely that electronic excitation would break the inversion symmetry of the molecule, it is more probable that the symmetric stretch would be active in the emission spectrum. Note that the $\nu = 1$ level of the $3u$ state cannot be clearly identified in the spectrum as it is overlapped by the low-frequency wing of the $1u$ band. We attribute the structure in the 392–416 nm range to transitions that terminate on excited vibrational levels of the $X^3\Phi_{2u}$, $^3\Phi_{3u}$, $^3\Delta_{1u}$, and $^3\Delta_{2u}$ states.

Chang's¹⁰ calculations provide two plausible candidates for the upper level of the near UV emission bands. The first is a state predicted to lie at a slightly higher energy ($33\,092\text{ cm}^{-1}$) that belongs to the U(5f ϕ_u 7p σ_u) configuration and has a wave function that is 77% $^3\Phi_{2g}$. The second candidate level, derived from U(5f ϕ_u 7p π_u), is at $26\,222\text{ cm}^{-1}$. It is composed of a mixture of singlet and triplet basis states (the leading terms are $48\%^1\Delta_{2g} + 30\%^3\Delta_{2g}$). It is apparent from both the energetics and the fluorescence decay kinetics that excitation of the UO₂ bands using wavelengths shorter than 360 nm proceeds via nonradiative relaxation processes. The observation that the near UV and visible emission exhibit the same slow decay rate for excitation at 355, 308, and 266 nm indicates that a common bottleneck is encountered in the paths to both states. The shorter lifetimes obtained using longer wavelength excitation are likely to be much closer to the intrinsic lifetimes of the emitting levels. Excitation at 308 and 266 nm was found to be more effective than excitation at 355 nm, which suggests that the shorter wavelengths accessed transitions that had greater oscillator strengths. Photons with $\lambda \leq 308$ nm may have enough energy to reach the U(5f ϕ_u 7p σ_u) $^3\Phi_{2g}$ state, while 355 nm light must

(12) Steinhaus, D. W.; Radziemski, L. J.; Cowan, R. D.; Blaise, J.; Guelachvili, G.; Osman, Z. B.; Verges, J. Report LA-4501, Los Alamos Sci. Lab., Los Alamos, NM, 1971, 243 pp.

(13) Kaledin, L. A.; McCord, J. E.; Heaven, M. C. *J. Mol. Spectrosc.* **1994**, *64*, 27.

(14) Kaledin, L. A.; Heaven, M. C. *J. Mol. Spectrosc.* **1997**, *185*, 1.

(15) Goncharov, V.; Han, J.; Kaledin, L. A.; Heaven, M. C. *J. Chem. Phys.*, in press.

(16) Jacox, M. E. *J. Mol. Struct.* **1987**, *157*, 43.

(17) Gabelnick, S. D.; Reedy, G. T.; Chasanov, M. G. *J. Chem. Phys.* **1973**, *58*, 4468.

rely on the weaker transition that excites $\text{U}(5f\phi_u7p\pi_u) \ ^1\Delta^3\Delta$ directly. Calculations for levels above $33\,092\text{ cm}^{-1}$ are not available, so we do not have information concerning the states that might be accessed by 266 nm excitation.

Excitation spectra show that the upper level of the visible emission band system lies at least 1190 cm^{-1} below the upper level of the near UV bands. Here, we consider two alternative assignment schemes for the visible bands, derived from the energy level calculations of Chang.¹⁰ First, we assume that the upper level is directly excited by 380.5 nm light. As the visible bands span the range from 470 to 600 nm (cf., Figure 1b), this assumption implies that the lower levels are $5000\text{--}9600\text{ cm}^{-1}$ above the $\text{X}^3\Phi_{2u}$ ground state. This is in reasonable agreement with the theoretical calculations that predict the following states (energies in cm^{-1} units given in parentheses): $3u(5398)$, $4u(5756)$, $2u(5864)$, and $3u(6514)$. The alternative interpretation is to assume that the upper level is populated by nonradiative transfer, which is then followed by radiative decay to the same group of lower levels that are accessed by the near UV emission bands. This interpretation would place the upper level of the visible bands at $21\,280\text{ cm}^{-1}$. Chang's¹⁰ calculations predict three plausible candidates for this level, all of which have good oscillator strengths for emission back to the ground state. The first two are a pair of $1g$ states at $20\,262$ and $20\,938\text{ cm}^{-1}$, which are both derived from admixtures of the $^3\Delta_{1g}(5f\phi_u7p\pi_u)$ and $^3\Sigma_{1g}(5f\phi_u^2)$ states. The third state ($^3\Pi_{1g}(5f\phi_u5f\delta_u) + ^1\Pi_{1g}(5f\pi_u5f\delta_u)$) is at $22\,190\text{ cm}^{-1}$. At present, we do not have enough information to determine whether 380.5 nm light excites the visible bands by a direct or indirect process.

The analysis presented so far is based on the assumption that the electronic structure calculations for gas-phase UO_2 will also be valid for UO_2 isolated in solid Ar. This is usually a good approximation, but, as noted in the Introduction, it has been suggested that the guest–host interaction in Ar matrices reorders the low-lying electronic states of UO_2 . Zhou et al.² propose that the ground state in Ar is $\text{U}(5f^2) \ ^3\text{H}$. The present results are not consistent with this assignment. As the ground state would change from u to g symmetry, we would not expect to be able to correlate the gas-phase and matrix excitation spectra, nor interpret the matrix emission spectra in terms of transitions to the lowest energy manifold of $\text{U}(5f7s) \ u$ states. The lowest energy states of the $\text{U}(5f^2)$ configuration are predicted to be the $\Omega = 4g, 5g,$ and $6g$ components of the ^3H term. In addition, there is a $^3\Pi_{1g}$ state just below $^3\text{H}_{6g}$ (which would not be optically accessible in an absorption-emission sequence that started from $\Omega = 4$). Chang's¹⁰ calculations yield splittings between the ^3H levels of $3850(5g-4g)$ and $3550\text{ cm}^{-1}(6g-5g)$. This same pattern of $\text{U}(5f^2)$ states was obtained by Gagliardi et al. (see Figure 2 of ref 8). Clearly, the resolved bands of UO_2 in the $370\text{--}390\text{ nm}$ range are not readily explained in terms of the $\text{U}(5f^2)$ energy levels.

From one perspective, it is not surprising to find that the ordering of the lowest energy UO_2 configurations is not reversed by $\text{UO}_2\text{--Ar}$ interactions. Ab initio calculations^{8,10} yield estimates for the energy separation between the $^3\Phi_{2u}$ and $^3\text{H}_{4g}$ states of 8389 and 4200 cm^{-1} . DFT calculations that did not include spin–orbit coupling² gave a $^3\Phi\text{--}^3\text{H}$ spacing of 1930 cm^{-1} . It seems unlikely that interactions with Ar would be able to

Table 2. Theoretical Predictions for the Stretching Vibrational Frequencies of UO_2

state	stretching frequency ^a		method	ref
	σ_g	σ_u		
$^3\Phi$	874	931	B3LYP	2
$^3\Phi$	896	913	MP2	9
$^3\Phi$	927	958	CCD	9
$^3\Phi_{2u}$	948	923	CASPT2/SO	8
^3H	792	814	B3LYP	2

^a In units of cm^{-1} .

produce such large differential shifts in the energies of the $^3\Phi$ and ^3H states. In this context, it is of interest to consider the analogous results for CUO . Spin-free DFT calculations yielded a closed-shell $^1\Sigma^+$ ground state with a $^3\Phi$ state just 240 cm^{-1} higher in energy.⁶ The C–UO stretching frequency was predicted to be 1049 and 902 cm^{-1} for the singlet and triplet states, respectively. Calculations for CUO--Ar at the same level of theory yielded $^3\Phi$ as the ground state, with a C–UO stretching frequency of 887 cm^{-1} . These results were used to account for the anomalous change in the C–UO vibrational frequency in going from Ne (1047.3 cm^{-1}) to Ar (852.5 cm^{-1}) matrices. Roos et al.¹⁸ raised doubts concerning this interpretation. They carried out ab initio calculations for CUO that included spin–orbit coupling (CASSCF/CASPT2/SO). At this level of theory, the spin–orbit interaction was found to be large for the triplet state, such that the $^3\Phi_2$ component lies about 4000 cm^{-1} below $^1\Sigma^+$ for unperturbed CUO . As the interaction with Ar stabilizes the triplet state relative to the singlet, this situation would not lead to state reordering in going from Ne to Ar matrices. However, the most recent ab initio calculations of Bursten et al.,¹⁹ carried out at the CCSD(T) level of theory, predict that the $^1\Sigma^+\text{--}^3\Phi$ splitting (5500 cm^{-1}) is large enough that spin–orbit coupling would not be able to push $^3\Phi_2$ below $^1\Sigma^+$. As the present results for UO_2 do not indicate a reordering of states in Ar, it is difficult to explain both the low vibrational frequencies observed in Ar and the Ne/Ar matrix shifts. Vibrational frequencies for UO_2 obtained from DFT and ab initio calculations are collected in Table 2. In all cases, the frequencies for $^3\Phi$ are significantly larger than the matrix results ($\sigma_g = 765$, $\sigma_u = 776\text{ cm}^{-1}$).

Aside from the question of state reordering, it is apparent, from the anomalous matrix shifts, that both UO_2 and CUO exhibit unusually strong interactions with Ar and heavier rare gas atoms. This is an intriguing phenomenon that deserves further experimental and theoretical attention.

Acknowledgment. We thank Dr. Leonid A. Kaledin and Professors Russell M. Pitzer, Laura Gagliardi, Björn O. Roos, Bruce E. Bursten, and Lester Andrews for several helpful discussions concerning the electronic structure of UO_2 . We also thank Prof. Pitzer for providing a copy of Qiang Chang's Masters thesis. This work was supported by the Department of Energy under grant DE-FG02-01ER15153-A001.

JA038940H

(18) Roos, B. O.; Widmark, P.-O.; Gagliardi, L. *Faraday Discuss.* **2003**, *124*, 57.

(19) Bursten, B. E.; Drummond, M. L.; Li, J. *Faraday Discuss.* **2003**, *124*, 57.